

# Fabrication and Characterization of Transparent Conductive ZnO:Al Thin Films Deposited on Polyethylene Terephthalate Substrates

Wei-Jen Yang,<sup>‡</sup> Chung-Chen Tsao,<sup>§</sup> Chun-Yoa Hsu,<sup>¶</sup> Hung-Chih Chang,<sup>¶</sup> Chang-Ping Chou,<sup>‡</sup>  
and Jin-Yih Kao<sup>¶,†</sup>

<sup>‡</sup>Department of Mechanical Engineering, National Chiao Tung University, Hsinchu City, Taiwan

<sup>§</sup>Department of Mechatronic Engineering, Tahua Institute of Technology, Hsinchu County, Taiwan

<sup>¶</sup>Department of Mechanical Engineering, Lunghwa University of Science and Technology, Taoyuan County, Taiwan

This article deals with the optimization of the process parameters, with regard to multiple performance characteristics, involved in the preparation of transparent conducting Al<sub>2</sub>O<sub>3</sub>-doped (2 wt.%) zinc oxide (AZO) thin films deposited onto flexible polyethylene terephthalate (PET) substrates, using radio frequency (RF) magnetron sputtering. Experiments based on the Grey-Taguchi method were conducted to examine the influence of deposition parameters (RF power, sputtering pressure, substrate-to-target distance, and coating time) on the deposition rate, electrical resistivity and structural, morphological and optical transmittance. Experimental results indicate that using the optimal parameter set selected by Grey theory prediction, it is possible to achieve an improvement of 3.8% in deposition rate, of 45.6% in resistivity, and to maintain the transmittance over 80%, compared to that achieved by using the Taguchi method. For the Grey theory prediction, films were deposited using substrate-to-target distance of 80, 85, and 90 mm, while maintaining constant values for the other conditions. A clear decrease in resistivity was observed, as substrate-to-target distance decreased, with the lowest resistivity being obtained at 80 mm, although a better optical transmittance was achieved at a distance of 85 mm. It is evident that the resistivity decreases as the Al buffer thickness increases, with the lowest resistivity  $7.0 \times 10^{-4} \Omega\text{-cm}$ , being found for a 15 nm thickness of Al buffer. The transmittance decreases, as the Al buffer thickness increases; transmittance values of 84.5%, 81.8%, and 79.4% correspond to an Al buffer thickness of 5, 10, and 15 nm, respectively. From the results of pull-off testing, the adhesive strength of the AZO film on a PET substrate increases, as the buffer thickness is increased.

## I. Introduction

TRANSPARENT conductive zinc oxide (ZnO) thin films have garnered much attention, because they are non-toxic, low-cost, and the materials are abundant.<sup>1</sup> Of impurity-doped ZnO films, aluminum-doped ZnO (AZO) is considered to be a viable alternative to indium tin oxide (ITO) and tin oxide (SnO<sub>2</sub>), owing to its high optical transmittance and low electrical resistivity.<sup>2,3</sup> Nowadays, polymer materials are taking the place of glass, as substrates for transparent conductive oxide (TCO) thin films. The polymer materials have more intrinsic flexibility, lighter weight, smaller volume, better impact resistance, and a better ability to withstand greater

strain than glass substrates.<sup>1,4</sup> Various techniques have been used to deposit the AZO films, but radio frequency (RF) magnetron sputtering is the most favored method,<sup>5</sup> due to its high reproducibility, the fact that it permits deposition at low temperature, and produces smooth films with a good surface uniformity.<sup>3</sup> In depositing the AZO films on polymer substrates by using RF magnetron sputtering, Hao *et al.*<sup>6</sup> pointed out that the crystallite sizes and the density of AZO films deposited on polypropylene adipate (PPA) substrates were increased and the resistivity was decreased, as film thickness was increased. Fortunato *et al.*<sup>4</sup> studied the mechanical properties of AZO films deposited on polyethylene terephthalate (PET) and concluded that the electrical resistance is related to the crack width, which is dependent on the film thickness. Lin *et al.*<sup>2</sup> investigated the effects of varying various parameters on the deposition of AZO films on flexible polyethersulfone (PES) substrates, reporting the influence of RF power, working pressure, and substrate bias on crystalline quality, conductivity, and transmittance. Antony *et al.*<sup>7</sup> have shown that the structural, electrical and optical properties of the films were related to the substrate-to-target distance.

Fernández *et al.*<sup>3,8</sup> optimized the deposition of AZO films on PET substrates and noted a resistivity as low as  $1.1 \times 10^{-3} \Omega\text{-cm}$  and a high value for transmittance, of  $\sim 80\%$ , for samples deposited at 100°C, 75 W and 0.2 Pa. Kim *et al.*<sup>9</sup> deposited 100 nm thick AZO films on polyethylene naphthalate (PEN) substrates and found that the resistivity decreases, as the sputtering power, substrate-to-target distance and working pressure increase, because of the improvement in crystallinity, due to larger grain size. The process of deposition of AZO films on polymer substrate should be geared toward obtaining a product of higher optical transmittance as well as lower electrical resistivity, while maintaining a high deposition rate. Therefore, it is important to properly select the process parameters to improve the film qualities.

On the other hand, many process parameters affect the quality characteristics of deposited substrates. Taguchi method can provide more efficient evaluation than the traditional factorial design in experiment with fewer trials and at lesser cost. However, Taguchi method was adopted in manufacturing to improve product or process design optimization with a single performance characteristic. Grey relational analysis can effectively be adopted as a method for optimizing the complicated inter-relationships among multiple performance characteristics. Through the Grey relational analysis, a Grey relational grade is obtained to evaluate the multiple performance characteristics. As a result, optimization of the complicated multiple performance characteristics can be converted into the optimization of a single Grey relational grade. Grey-based Taguchi method was established for combining both Grey relational analysis and Taguchi method. This article, aims to optimize the process parameters

J. McKittrick—contributing editor

Manuscript No. 30321. Received September 23, 2011; approved February 28, 2012.

<sup>†</sup>Author to whom correspondence should be addressed. e-mail: jykao@mail.lhu.edu.tw

relevant to the production of transparent conductive AZO (ZnO:Al = 98:2 wt%) thin films on a PET substrate (TORAY Lumirror<sup>®</sup> T60, Toray Industries, Inc., Tokyo, Japan) using RF magnetron sputtering. The influence on the thin film qualities of the substrate-to-target distance and the thickness of Al buffer layer are also discussed.

## II. Experimental Details

Using a ZnO:Al ceramic target (50.8 mm in diameter), AZO thin films were deposited on PET substrates by DC 150W RF reactive magnetron sputtering with a base pressure of  $0.67 \times 10^{-3}$  Pa. The sputtering gas was Ar (purity: 99.995%). The flow rate of argon was controlled by mass flow meters and the sputtering pressure was measured using an ion gauge. The high purity Al target was placed in an Ar atmosphere, with a fixed working pressure of 5.33 Pa. The distance between substrate and target was 80 mm. During deposition, the substrates were rotated at 10 rpm to achieve film thickness uniformity. The PET substrates are cut into coupon specimens of 25 mm  $\times$  25 mm  $\times$  1 mm.

The AZO films' deposition conditions are shown in Table I; four process parameters (RF power, sputtering pressure, substrate-to-target distance, and coating time) were selected as the control factors and each had three levels (Level 1, Level 2, and Level 3), through which they could be varied. A Taguchi experimental design, with an  $L_9$  ( $3^4$ ) orthogonal array, of four columns and nine rows, governed the experiments.<sup>10</sup> Each test was replicated twice. The deposition rate (Dr1 and Dr2), electrical resistivity (Er1 and Er2), and optical transmittance (Ot1 and Ot2) were the performance characteristics used to evaluate the film quality. Before the coating process, the PET substrates were ultrasonically cleaned in acetone, rinsed in de-ionized water and dried in nitrogen. On the other hand, Al thin films were grown on a PET substrate at room temperature as the buffer layer to investigate their influence on the qualities of the AZO film in this study. The target Al (99.995% purity), 150 W DC power, 30 kHz pulse frequency, 3  $\mu$ s pulse time and Al buffers of thickness 5, 10 and 15 nm, respectively, were used. A surface profilometer ( $\alpha$ -step; ET-4000A) was used to measure the thickness of the deposited AZO film. Electrical resistivity was measured using the four-point probe method (Mitsubishi Chemical MCP-T600, Mitsubishi Chemical Corporation, Tokyo, Japan). The structure of the film was determined using X-ray diffraction (XRD) (Rigaku-2000 X-ray Generator, Rigaku Corporation, Tokyo, Japan), using  $CuK\alpha$  radiation, with an angle of incidence of  $1^\circ$ . Surface morphology was analyzed using a JEOL JSM-6500F (JOEL Ltd., Tokyo, Japan) field emission scanning electron microscope (FESEM). The optical transmittance measurement was performed using a UV-VIS spectrophotometer in the wavelength range from 300 to 800 nm.

### (1) Analysis of the Single to Noise (S/N) Ratio

The S/N ratio transforms several repetitions into one value which reflects the amount of variation present and the mean response.<sup>10</sup> The concept of S/N ratio is useful to improve the quality of products or processes via variability reduction and

the improvement of measurement. In this study, deposition rate and optical transmittance represent the higher the better (HB) category of performance characteristics for the Taguchi method, and the electrical resistivity is the lower, the better (LB) characteristic. The S/N ratios of LB and HB can be calculated as follows<sup>11,12</sup>:

$$\eta = 10 \log(S/N \text{ ratio}) \quad (1)$$

$$HB:(S/N \text{ ratio}) = \frac{1}{\sigma^2}, \quad \sigma^2 = \frac{1}{n} \sum_{j=1}^n \frac{1}{y_j^2} \quad (2)$$

$$LB:(S/N \text{ ratio}) = \frac{1}{\sigma^2}, \quad \sigma^2 = \frac{1}{n} \sum_{j=1}^n y_j^2 \quad (3)$$

where  $\eta$  denotes the S/N ratio of LB or HB characteristic (unit: dB),  $n$  is the number of repetitions of the experiment ( $n = 9$ ) and  $y_j$  is the average measured value of experimental data  $j$ .

### (2) Analysis of Variance

ANOVA is used to analyze the experimental data, to investigate which coating parameters significantly affect the performance characteristics.<sup>11,12</sup>

$$S_m = \frac{(\sum \eta_i)^2}{9}, \quad S_T = \sum \eta_i^2 - S_m \quad (4)$$

$$S_Z = \frac{(\sum \eta_{Zi}^2)}{N} - S_m, \quad S_E = S_T - \sum S_Z \quad (5)$$

$$V_Z = \frac{S_Z}{f_Z}, \quad F_{Z0} = \frac{V_Z}{V_E} \quad (6)$$

where  $S_T$  is the sum of the squares due to the total variation,  $S_m$  is the sum of squares due to the means,  $S_Z$  is the sum of squares due to parameter  $Z$  ( $Z =$  RF power, sputtering pressure, substrate-to-target distance and coating time).  $S_E$  is the sum of squares due to error,  $\eta_i$  is the  $\eta$  value of each experiment ( $i = 1-9$ ),  $\eta_{Zi}$  is the sum of the  $i^{\text{th}}$  level of parameter  $Z$  ( $i = 1, 2, 3$ ),  $N$  is the repeating number of each level of parameter  $Z$ ,  $f_Z$  is the degree of freedom of parameter  $Z$ ,  $V_Z$  is the variance of parameter  $Z$  and  $F_{Z0}$  is the  $F$ -test value of parameter  $Z$ .

## III. Grey Relational Analysis

Using Grey relational analysis to consider the multiple performance characteristics, the Grey relational coefficient and Grey relational grade must be sequentially calculated from the normalized S/N ratio.<sup>13</sup> The Grey relational coefficient is given below<sup>14</sup>:

$$r(x_0(k), x_i(k)) = \frac{\min_i \min_k |x_0(k) - x_i(k)| + \zeta \max_i \max_k |x_0(k) - x_i(k)|}{|x_0(k) - x_i(k)| + \zeta \max_i \max_k |x_0(k) - x_i(k)|} \quad (7)$$

where  $x_i(k)$  is the normalized value of the  $k^{\text{th}}$  performance characteristic in the  $i^{\text{th}}$  experiment,  $\zeta$  is the distinguishing coefficient and  $\zeta \in [0, 1]$ . The value of  $\zeta$  can be adjusted, according to the actual system requirement. In this article, the AZO deposition process parameters are equally weighted, therefore  $\zeta$  is 0.5. The Grey relational grade is a weighting-sum of the Grey relational coefficient, corresponding to each performance characteristic. It is defined as follows<sup>14</sup>:

**Table I. Deposition Parameters of AZO Films**

Symbol	Parameter	Level		
		1	2	3
A	RF power (W)	40	80	120
B	Sputtering pressure (Pa)	0.67	1.33	2.0
C	Substrate-to-target distance (mm)	70	85	100
D	Coating time (min)	30	60	90

$$r(x_0, x_i) = \frac{1}{ns} \sum_{k=1}^{ns} r(r_0(k), x_i(k)) \quad (8)$$

where  $ns$  is the number of performance characteristics. The Grey relational grade shows the correlation between the reference sequence and the comparability sequence, to which it is compared. The evaluated Grey relational grade fluctuates from 0 to 1, and equals 1 if these two sequences are identically coincident.

#### IV. Results and Discussion

Table II shows the experimental results of the deposition rate, electrical resistivity, and optical transmittance, and the corresponding S/N ratios using Eqs. (2) and (3), respectively. The ANOVA results for the deposition rate, electrical resistivity, and optical transmittance are listed in Table III. Table III shows that the RF power is crucial to the AZO deposition rate, with a highest contribution of 69.4%. The deposition rate increases, as the RF power increases. The ions or the ion clusters are imbued with a higher energy by a higher sputtering power, which helps nucleation and growth. It also causes the AZO films to be deposited at a gradually increased substrate temperature, owing to the effect of bombardment by higher energy particles. These effects not only

enhance the growth process occurs, but also produce a film with increased grain size.<sup>15</sup> The experimental results also reveal that decreasing the substrate-to-target distance increases the deposition rate. This observation is similar to that noted in the reports by Jeong *et al.*<sup>16</sup> It seems probable that the mean free path is comparable to the substrate-to-target distance, so particles arriving at the surface have high mobility, allowing greater growth to occur.<sup>17</sup>

From Table III, it can be seen from the ANOVA results that substrate-to-target distance is the most significant factor to influence the resistivity, with a contribution of nearly 79.0%. The resistivity decreases when the distance between substrate and target decreases, which means that films of lower resistivity were produced by decreasing the distance from 100 to 70 mm. This effect results from the improved crystallinity, which reduces the grain boundary scattering, to charge carriers, so the electrical resistivity decreases.<sup>16</sup>

From Table III, it can be seen that substrate-to-target distance (with a 47.0% contribution) and sputtering pressure (with a 34.5% contribution) have a statistically and, in turn, a physically significant effect on the optical transmittance. As can be seen in the S/N response for optical transmittance, shown in Table III, a substrate-to-target distance of 85 mm and a higher sputtering pressure, of 2.0 Pa, increases the optical transmittance of AZO films deposited on PET substrates.

**Table II. Experimental Results and S/N Ratios for Deposition Rate, Electrical Resistivity, and Optical Transmittance in the AZO Deposition**

Exp.	Factors				Composition	Deposition rate (nm/min)			Electrical resistivity ( $10^{-3}$ $\Omega$ -cm)			Optical transmittance (%)		
	A	B	C	D		Dr1	Dr2	S/N (dB)	Er1	Er2	S/N (dB)	Ot1	Ot2	S/N (dB)
1	40	0.67	70	30	A <sub>1</sub> B <sub>1</sub> C <sub>1</sub> D <sub>1</sub>	5.1	5.4	14.4	19.0	18.0	-25.3	77.3	77.2	37.8
2	40	1.33	85	60	A <sub>1</sub> B <sub>2</sub> C <sub>2</sub> D <sub>2</sub>	4.8	5.6	14.3	16.0	14.0	-23.5	77.9	78.1	37.8
3	40	2.0	100	90	A <sub>1</sub> B <sub>3</sub> C <sub>3</sub> D <sub>3</sub>	2.9	2.7	8.9	36.0	35.0	-31.0	78.7	78.5	37.9
4	80	0.67	85	90	A <sub>2</sub> B <sub>1</sub> C <sub>2</sub> D <sub>3</sub>	7.5	7.6	17.6	16.0	17.0	-24.3	80.2	80.4	38.1
5	80	1.33	100	30	A <sub>2</sub> B <sub>2</sub> C <sub>3</sub> D <sub>1</sub>	7.0	7.3	17.1	51.0	53.0	-34.3	76.0	76.3	37.6
6	80	2.0	70	60	A <sub>2</sub> B <sub>3</sub> C <sub>1</sub> D <sub>2</sub>	9.0	8.8	19.0	6.8	6.6	-16.5	78.4	78.1	37.9
7	120	0.67	100	60	A <sub>3</sub> B <sub>1</sub> C <sub>3</sub> D <sub>2</sub>	9.7	9.2	19.5	39.0	37.0	-31.6	74.1	74.6	37.4
8	120	1.33	70	90	A <sub>3</sub> B <sub>2</sub> C <sub>1</sub> D <sub>3</sub>	14.9	15.6	23.7	5.5	5.2	-14.6	73.8	73.9	37.4
9	120	2.0	85	30	A <sub>3</sub> B <sub>3</sub> C <sub>2</sub> D <sub>1</sub>	7.9	7.2	17.6	13.0	11.0	-21.6	81.0	80.9	38.2

**Table III. ANOVA Results for Deposition Rate, Electrical Resistivity, and Optical Transmittance in the AZO Deposition**

Factor	S/N ratio (dB)			Degree of freedom	Sum of square	Variance	Contribution (%)
	Level 1	Level 2	Level 3				
<b>Deposition rate</b>							
A	12.6	17.9	20.2	2	93.0	46.5	69.4
B	17.2	18.4	15.2	2	15.6	7.8	11.6
C	19.0	16.5	15.2	2	22.9	11.4	17.1
D	16.4	17.6	16.7	2	2.5	1.2	1.9
Total				8	134.0		100
<b>Electrical resistivity</b>							
A	-26.6	-25.1	-22.6	2	24.9	12.4	6.9
B	-27.1	-24.1	-23.0	2	26.4	13.2	7.3
C	-18.8	-23.2	-32.3	2	284.8	142.4	78.9
D	-27.1	-23.9	-23.3	2	24.8	12.4	6.9
Total				8	361.016		100
<b>Optical transmittance</b>							
A	37.8	37.9	37.7	2	0.080	0.040	13.5
B	37.8	37.6	38.0	2	0.205	0.102	34.5
C	37.7	38.0	37.7	2	0.279	0.139	47.0
D	37.9	37.7	37.8	2	0.029	0.014	5.0
Total				8	0.593		100



### (1) Determination of Optimal Deposition Parameters

In this study, deposition rate, electrical resistivity, and optical transmittance were considered to be the key performance characteristics. However, they can be converted into a single Grey relational grade by means of Eqs. (7) and (8). The Grey relational grade for each AZO deposition experiment in the  $L_9 (3^4)$  orthogonal array is shown in Table IV. The larger the Grey relational grade, which represents the corresponding experimental result that is closer to the ideal normalized value, the better will be the key performance characteristics. It can be seen that experiment 9 in the Table IV shows the highest Grey relational grade, indicating that the parameter set of  $A_3B_3C_2D_1$  has the best combination of performance characteristics of the nine experiments. The effect of each deposition process parameter on the Grey relational grade at different levels can be isolated, because the experimental design is orthogonal. Table V shows that the predicted optimal process parameter set, based on the Grey theory, is  $A_3B_3C_2D_3$ , because this optimal process parameter set is the combination of levels with the highest Grey relational grade.

### (2) Confirmation Tests

Since the optimal parameter set for the AZO deposition process was selected, the confirmation tests were performed to verify any improvement. Table VI compares the multiple performance characteristics for the optimal parameter set ( $A_3B_3C_2D_1$ ) in the orthogonal array with the Grey theory prediction ( $A_3B_3C_2D_3$ ) for the AZO deposition process. The results show an improvement of 3.8% in deposition rate, increasing from 7.9 to 8.2 nm/min, an improvement of 45.6% in resistivity, decreasing from  $12.5 \times 10^{-3} \Omega\text{-cm}$  to  $6.8 \times 10^{-3} \Omega\text{-cm}$ , and a slight increase in transmittance, from 81.0% to 83.1%. These results are consistent with the SEM micrographs of AZO films seen in Fig 1, and correspond to the X-ray diffraction spectrum in Fig. 2. Using the Grey theory prediction [Fig. 2(b)], the XRD pattern reveals that (002) peak becomes more intense and the full width at half maximum (b:FWHM) decreases from 0.446 to 0.381, compared with use of the orthogonal array parameters [Fig. 2(a)]. This shows that larger crystallite size of the deposited AZO films resulted in decreased resistivity ability using the Grey theory prediction (Fig. 1).

**Table IV. Grey Relational Grades and Their Orders, for the Optimization Process**

Exp.	Grey relational grade	Order
1	0.565	6
2	0.627	5
3	0.519	7
4	0.761	2
5	0.379	9
6	0.757	3
7	0.385	8
8	0.667	4
9	0.883	1

**Table V. Mean Value of the Grey Relational Grade, for Each Deposition Parameter Level**

	A	B	C	D
Level 1	-4.907	-5.209	-3.636	-4.824
Level 2	-4.406	-5.334	-2.505	-4.923
Level 3	-4.298	-3.068	-7.470	-3.864
Effect	0.610	2.266	4.964	1.059
Rank	4	2	1	3

**Table VI. Results of the Confirmation Test for Multiple Performance Characteristics, for the AZO Deposition Process**

	Orthogonal array process parameters	Grey theory prediction design	Improvement (%)
Optimize deposition condition	$A_3 B_3 C_2 D_1$	$A_3 B_3 C_2 D_3$	
Deposition rate (nm/min)	7.9	8.2	3.8
Resistivity ( $10^{-3} \Omega\text{-cm}$ )	12.5	6.8	45.6
Transmittance (%)	81.0	83.1	2.6

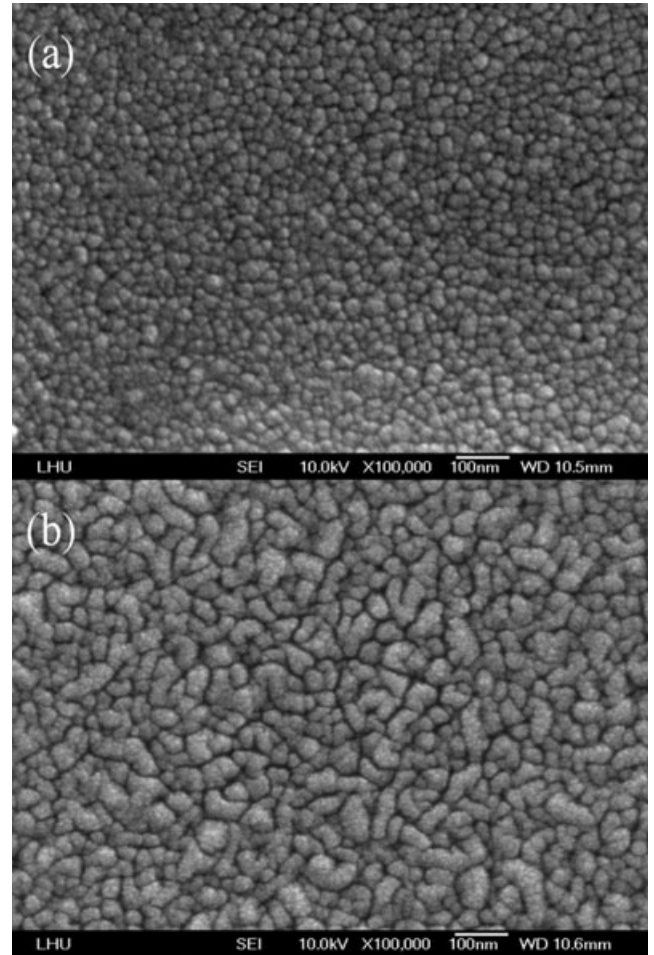


**Fig. 1.** SEM micrographs for AZO deposited on a PET substrate, using (a) Orthogonal array parameters ( $A_3B_3C_2D_1$ ) and (b) the Grey theory prediction ( $A_3B_3C_2D_3$ ).

### (3) Effect of Substrate-to-Target Distance

The mean value of the Grey relational grade for each deposition parameter, in Table V, shows that the substrate-to-target distance is the most significant factor for both the resistivity and transmittance. To ascertain the effect of substrate-to-target distance, distances of 80, 85, and 90 mm were used while other variables in Grey theory prediction were fixed. Figure 3 shows the dependence of the resistivity and transmittance of the AZO films for Grey theory prediction on the substrate-to-target distance. The lowest resistivity, obtained by this study, was found for a substrate-to-target distance of 80 mm. A clear increase in resistivity is observed, as the substrate-to-target distance increases. This behavior can be ascribed to the increase in the crystallite (Fig. 4),

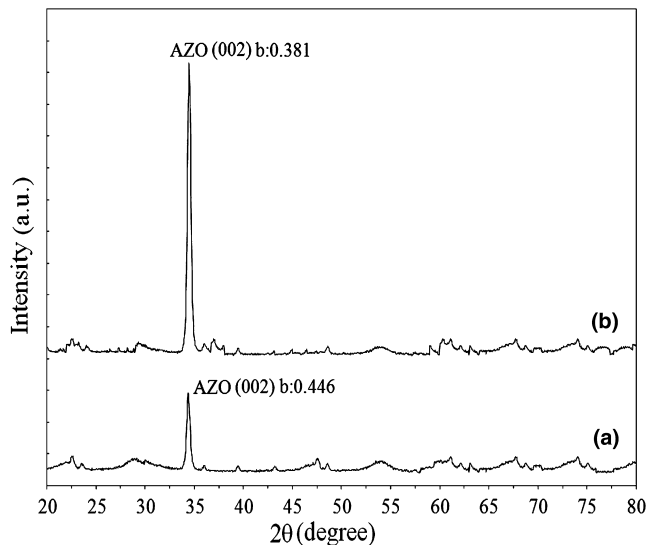


Fig. 2. XRD patterns for AZO deposited on a PET substrate, using (a) Orthogonal array parameters ( $A_3B_3C_2D_1$ ) and (b) the Grey theory prediction ( $A_3B_3C_2D_3$ ).

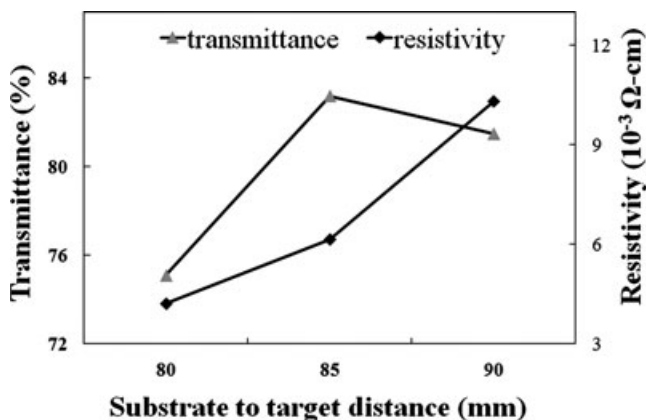


Fig. 3. The resistivity and transmittance for AZO thin films deposited on a PET substrate for Grey theory prediction, as a function of substrate-to-target distance.

which results in a lower value for resistivity.<sup>16</sup> As shown in Fig. 3, the films of substrate-to-target distance for a distance over 85 mm were highly transparent. However, a better optical transmittance was achieved in the films deposited at substrate-to-target distance of 85 mm in comparison with the other two substrate-to-target distance. So the discussion regarding the variation of optical transmittance on Grey theory prediction is limited to the case of substrate-to-target distance of 85 mm only.

#### (4) Effect of Al Buffer Layer

A buffer layer, incorporated between the film and the substrate, has been reported to improve the crystallinity and structure of the film.<sup>18</sup> However, the thickness of buffer layer is very important for the performance characterizations of films because the match in the lattice structure between a film and a substrate strongly affects the crystalline quality of films. Bang *et al.*<sup>19</sup> also pointed out that the surface morphology and structural and optical properties of the films depend on the thickness of the buffer layer. The AZO films were then deposited using the parameters from the Grey theory prediction ( $A_3B_3C_2D_3$ ). The resistivity of AZO thin films as a function of Al buffer thickness is shown in Fig. 5. It is evident that the resistivity decreases as the Al buffer thickness increases, and the lowest resistivity of  $7.0 \times 10^{-4} \Omega\text{-cm}$

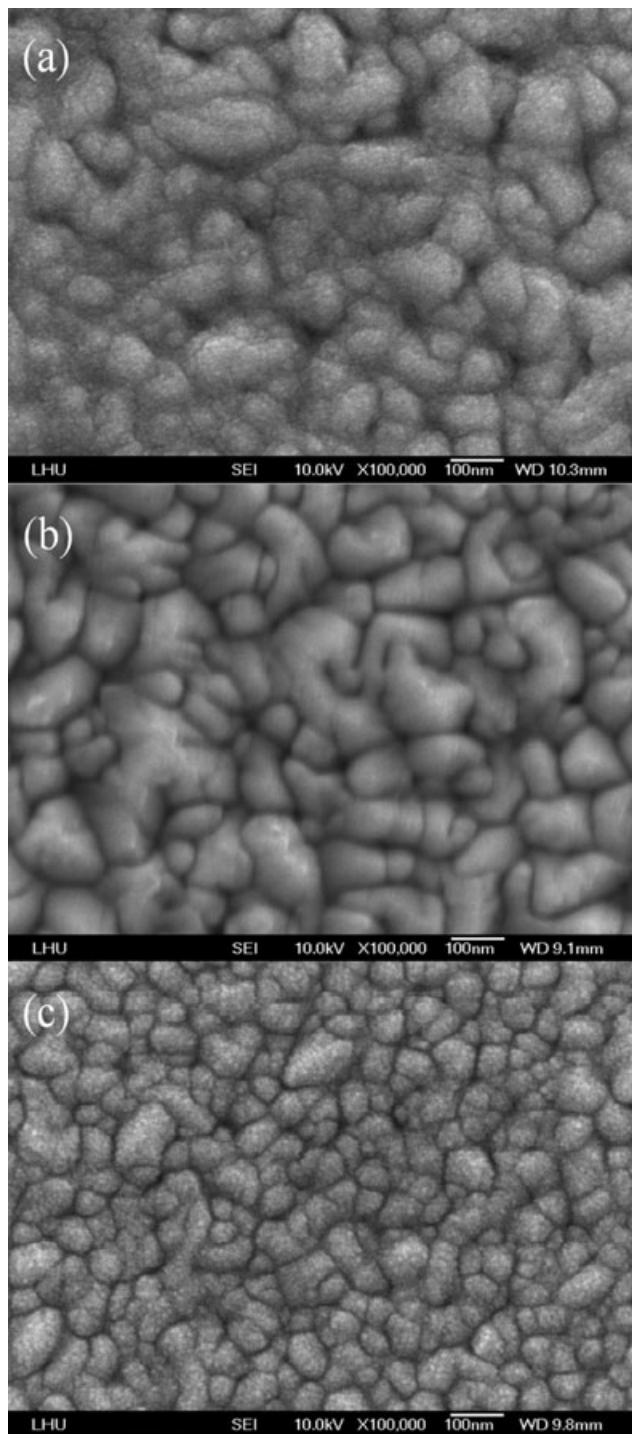


Fig. 4. SEM micrographs for AZO thin films deposited on a PET substrate for Grey theory prediction at different substrate-to-target distances (a) 80 mm, (b) 85 mm and (c) 90 mm.

occurs at a 15 nm thickness of Al buffer. Figure 6 shows the XRD patterns of AZO films for various thickness of Al buffer. It shows that all the AZO films have a hexagonal ZnO wurtzite structure with a preferential orientation along the c-axis perpendicular to the substrate surface. For a thickness of Al buffer of 15 nm, the diffraction peaks of AZO films are sharper and more intense. This is due to an increase in crystallite size and an improvement in the crystallinity of the films.<sup>20</sup> It is also possible that the presence of the Al buffer increases the carrier concentrations and reduces the resistance of the film, since Al has a high diffusion coefficient and can migrate quickly into the AZO film during the deposition process.<sup>21</sup>

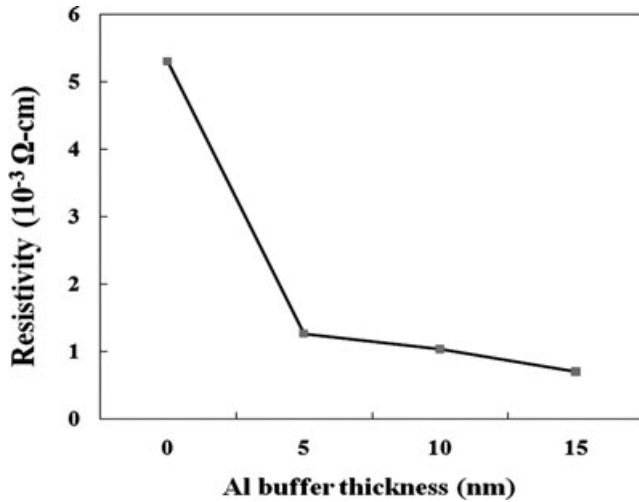


Fig. 5. The resistivity as a function of Al buffer thickness for AZO thin films, deposited on a PET substrate for Grey theory prediction.

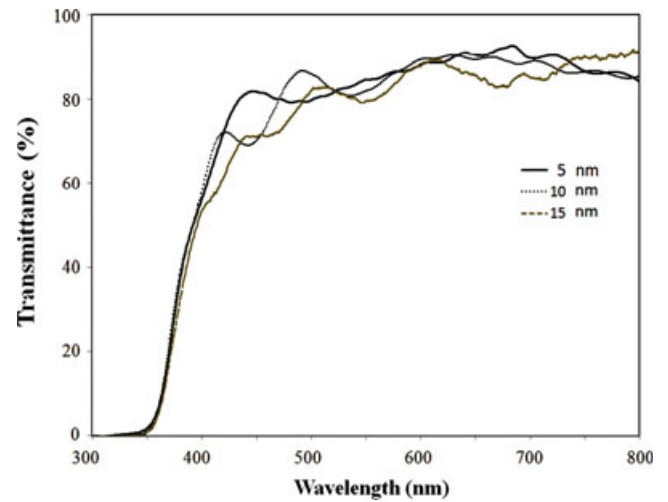


Fig. 7. Optical transmittance for AZO films, as a function of Al buffer thickness.

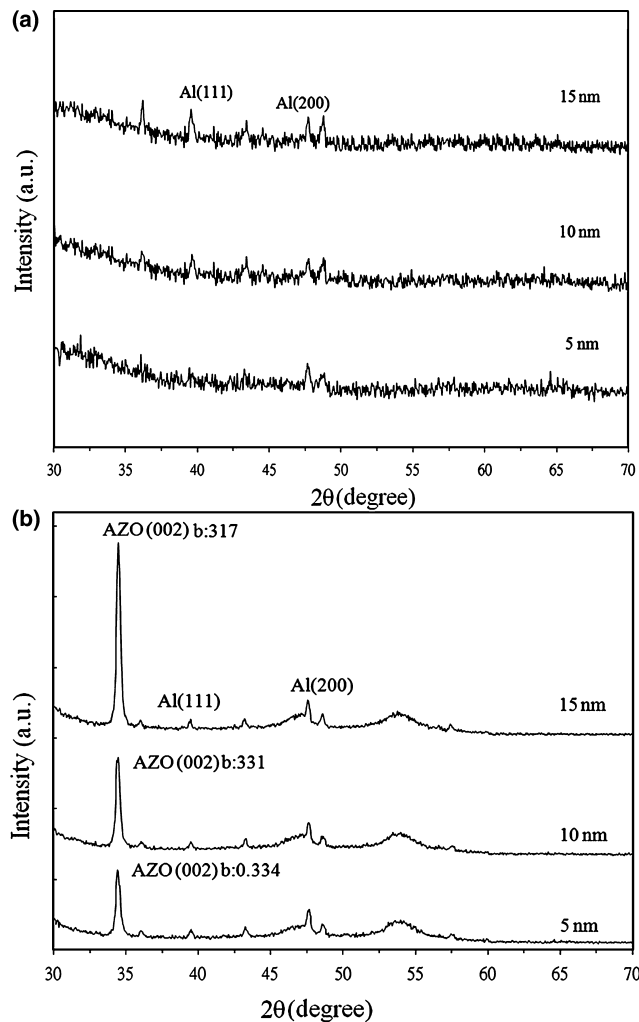


Fig. 6. X-ray diffraction (b: FWHM) for (a) Al buffer and (b) AZO/AI/PET.

The thickness of the metal layer (Au, Ag, and Al) is not allowed beyond a certain threshold for high transmittance. For thicker Ag layers (10 nm) reduced transmission is due to the absorption in the aggregated Ag film.<sup>21</sup> Figure 7 shows the experimental results for optical transmittance at different thicknesses of Al buffer layer in the wavelength range from

300 to 800 nm. It is observed that transmittance decreases as the thickness of the Al buffer increases; Al buffer thicknesses of 5, 10, and 15 nm, produce values of transmittance of 84.5%, 81.8%, and 79.4%, respectively. Figure 8 shows the transmittance of AZO films for different Al buffer thicknesses, compared to those without an Al buffer.

#### (5) Adhesion Testing

Good adherence is essential for films coated on polymeric substrates, because the flexible materials may encounter repeated folds. For AZO films deposited on PET substrates, Tseng *et al.*<sup>22</sup> measured adhesive strength with and without an Al buffer layer, using a pull-off adhesion test. The results indicated that AZO film on PET with an Al buffer layer exhibits a better adhesive strength than that without the buffer layer. In this study, the same tensile test was used to investigate the influence of buffer thickness on adhesive strength. A schematic diagram of the pull-off adhesion test, based on the direct tensile test method, is depicted in Fig. 9(a). Adhesive epoxy (3M Scotch-Weld, Epoxy adhesives DP-460) was applied between a 5-mm diameter steel bar and the AZO thin film. The pull testing was done at atmospheric pressure, room temperature and at a pulling speed of 1 mm/min. The photograph in Fig. 9(b) shows the difference after the pull-off testing; where zone 1 is the original area and zone 2 is the fracture surface of the AZO film. Tests were repeated twice and the results are presented in Table VII. It can be seen that, without Al buffer layer the peel off stress for the AZO film on a PET substrate is 12.7 MPa, but the stress dramatically increases to 21.3 MPa when 5 nm thick of Al buffer layer is added. The stress increases to 22.3 and 23.6 MPa, respectively, when the thickness of Al buffer is 10 and 15 nm.

#### V. Conclusion

This article presents optimized process parameters, using the  $L_9 (3^4)$  orthogonal array Taguchi method combined with Grey theory, for the production of AZO thin films on PET substrate. Multiple performance characteristics, including deposition rate, optical transmittance, and electrical resistivity were considered. The results show that the RF power is crucial to the deposition rate and that the substrate-to-target distance is a significant factor to both the electrical resistivity and optical transmittance. Using the optimal parameters from Grey theory prediction, an improvement of 3.8% in deposition rate, of 45.6% in resistivity, and 2.6% in transmittance was noted, compared to that produced by the



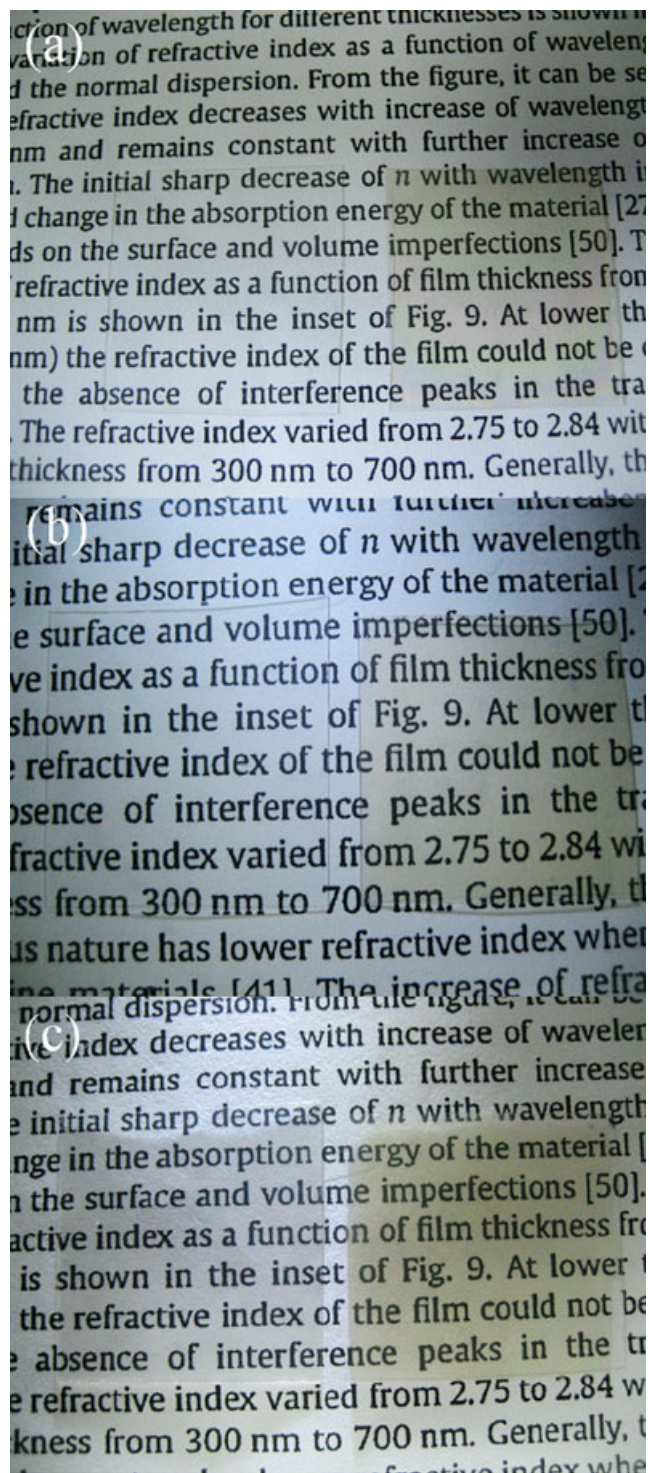


**Fig. 8.** Optical transmittance for the AZO/PET, without Al buffer, (left side) and that for AZO film grown on different thicknesses of Al buffer (right side): (a) AZO/Al 5 nm/PET, 84.5% transmittance; (b) AZO/Al 10 nm/PET, 81.8% transmittance, and (c) AZO/Al 15 nm/PET, 79.4% of transmittance.

Taguchi method. Using Grey theory prediction, films deposited at substrate-to-target distance of 80, 85, and 90 mm whereas other variables remained fixed; a clear increase in resistivity was observed as substrate-to-target distance was increased and the lowest resistivity occurred for a substrate-to-target distance of 80 mm, but a better optical transmittance was achieved, for a distance of 85 mm. It is evident that the resistivity of the Al buffer layer decreases as the Al buffer thickness increases; the lowest resistivity of

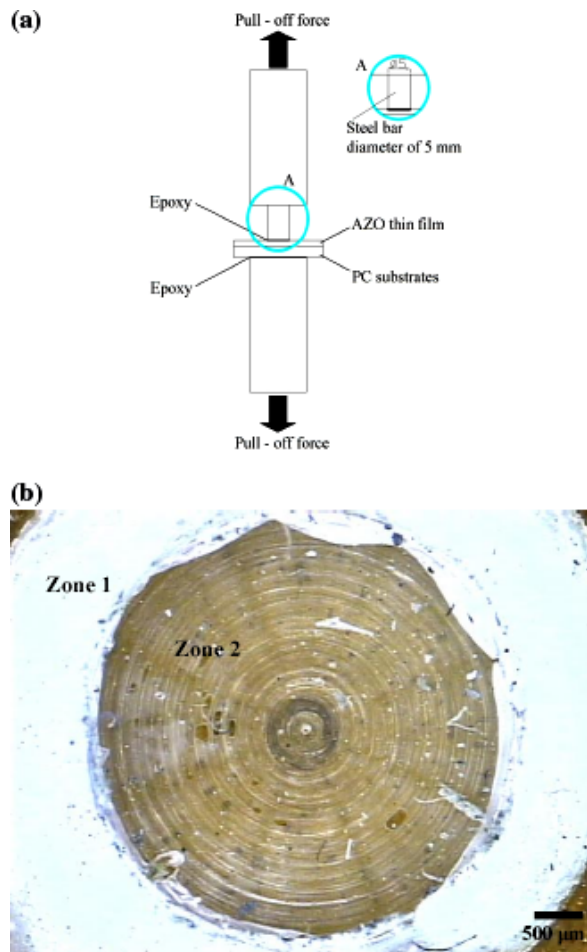


**Fig. 9.** (a) Schematic diagram of the pull-off adhesion test, (b) Photograph of AZO films (zone 1) and fracture surface (zone 2), after mechanical test (50 $\times$ ).

**Table VII.** Adhesive Strength of AZO/Al/PET Films at Different Thicknesses of Al Buffer Layer

	Maximum loading (kgf)	Maximum displacement (mm)	Peel off stress (MPa)
AZO without buffer layer	9.9	0.098	12.7
AZO/Al 5 nm/PET	12.4	0.101	21.3
AZO/Al 10 nm/PET	13.6	0.123	22.3
AZO/Al 15 nm/PET	14.8	0.116	23.6

$7.0 \times 10^{-4} \Omega\text{-cm}$  occurs at a thickness of Al buffer of 15 nm. The transmittance decreases as Al buffer thickness increases, with transmittance values of 84.5%, 81.8%, and 79.4% for Al buffer thicknesses of 5, 10, and 15 nm, respectively. From the results of pull-off testing, it is seen that the adhesive strength of an AZO film on a PET substrate dramatically increases when the Al buffer layer is added. Therefore, carefully selected deposition conditions produce higher optical transmittance as well as lower electrical resistivity on a PET substrate when using Grey-based Taguchi method.

## References

- C. S. Moon, Y. M. Chung, W. S. Jung, and J. G. Han, "The Low Temperature Process Design for Al Doped ZnO Film Synthesis on Polymer," *Surf. Coat. Technol.*, **201**, 5035–8 (2007).

- <sup>2</sup>Y. C. Lin, M. Z. Chen, C. C. Kuo, and W. T. Yen, "Electrical and Optical Properties of ZnO:Al Film Prepared on Polyethersulfone Substrate by RF Magnetron Sputtering," *Colloids Surf. A Physicochem. Eng. Aspects*, **337**, 52–6 (2009).
- <sup>3</sup>S. Fernández, A. Martínez-Steele, J. J. Gandía, and F. B. Naranjo, "Radio Frequency Sputter Deposition of High-Quality Conductive and Transparent ZnO:Al Films on Polymer Substrates for Thin Film Solar Cells Applications," *Thin Solid Films*, **517**, 3152–6 (2009).
- <sup>4</sup>E. Fortunato, P. Nunes, A. Marques, D. Costa, H. Águas, I. Ferreira, M. E. V. Costa, M. H. Godinho, P. L. Almeida, J. P. Borges, and R. Martins, "Transparent, Conductive ZnO:Al Thin Film Deposited on Polymer Substrates by RF Magnetron Sputtering," *Surf. Coat. Technol.*, **151–152**, 247–51 (2002).
- <sup>5</sup>O. Kluth, G. Schöpe, B. Rech, R. Menner, M. Oertel, K. Orgassa, and H. W. Schock, "Comparative Material Study on RF and DC Magnetron Sputtered ZnO:Al Films," *Thin Solid Films*, **502**, 311–6 (2006).
- <sup>6</sup>H. Hao, J. Ma, D. Zhang, T. Yang, H. Ma, Y. Yang, C. Cheng, and J. Huang, "Thickness Dependence of Structural, Optical and Electrical Properties of ZnO:Al Films Prepared on Flexible Substrates," *Appl. Surf. Sci.*, **183**, 137–42 (2001).
- <sup>7</sup>A. Antony, M. Nisha, R. Manoj, and M. K. Jayaraj, "Influence of Target to Substrate Spacing on the Properties of ITO Thin Films," *Appl. Surf. Sci.*, **225**, 294–301 (2004).
- <sup>8</sup>S. Fernández and F. B. Naranjo, "Optimization of Aluminum-Doped Zinc Oxide Films Deposited at Low Temperature by Radio-Frequency Sputtering on Flexible Substrates for Solar Cell Applications," *Sol. Energ. Mater. Sol. Cell*, **94** [2] 157–63 (2010).
- <sup>9</sup>J. M. Kim, P. Thiyagarajan, and S. W. Rhee, "Deposition of Al-Doped ZnO Films on Polyethylene Naphthalate Substrate with Radio Frequency Magnetron Sputtering," *Thin Solid Films*, **518**, 5860–5 (2010).
- <sup>10</sup>S. H. Park, *Robust Design and Analysis for Quality Engineering*, Chapman and Hall, New York, 1996.
- <sup>11</sup>J. Y. Kao, C. C. Tsao, S. S. Wang, and C. Y. Hsu, "Optimization of the EDM Parameters on Machining Ti-6Al-4V with Multiple Quality Characteristics," *Int. J. Adv. Manuf. Technol.*, **47**, 395–402 (2010).
- <sup>12</sup>Y. S. Tarng, S. C. Juang, and C. H. Chang, "The use of Grey-Based Taguchi Methods to Determine Submerged Arc Welding Process Parameters in Hard Facing," *J. Mater. Process. Technol.*, **128**, 1–6 (2002).
- <sup>13</sup>J. Deng, "Introduction to Grey System," *J. Grey Syst.*, **1** [1] 1–24 (1989).
- <sup>14</sup>J. Deng, "Control Problems of Grey Systems," *Syst. Contr. Lett.*, **5**, 288–94 (1982).
- <sup>15</sup>D. H. Zhang, T. L. Yang, J. Ma, Q. P. Wang, R. W. Gao, and H. L. Ma, "Preparation of Transparent Conducting ZnO:Al Films on Polymer Substrates by r.f. Magnetron Sputtering," *Appl. Surf. Sci.*, **158**, 43–8 (2000).
- <sup>16</sup>S. H. Jeong and J. H. Boo, "Influence of Target-to-Substrate Distance on the Properties of AZO Films Grown by RF Magnetron Sputtering," *Thin Solid Films*, **447–448**, 105–10 (2004).
- <sup>17</sup>J. A. Thornton, "Influence of Apparatus Geometry and Deposition Condition the Structure and Topography of Thick Sputtered Coatings," *J. Vac. Sci. Technol. A*, **11**, 660–70 (1974).
- <sup>18</sup>Y. Zhang, H. Zheng, J. Su, B. Lin, and Z. Fu, "Effects of sic Buffer Layer on the Optical Properties of ZnO Films Grown on Si (1 1 1) Substrates," *J. Luminescence*, **124**, 252–6 (2007).
- <sup>19</sup>K. H. Bang, D. K. Hwang, and J. M. Myoung, "Effects of ZnO Buffer Layer Thickness on Properties of ZnO Thin Films Deposited by Radio-Frequency Magnetron Sputtering," *Appl. Surf. Sci.*, **207**, 359–64 (2003).
- <sup>20</sup>E. Fortunato, A. Goncalves, V. Assuncao, A. Marques, H. Aguas, L. Pereira, I. Ferreira, and R. Martins, "Growth of ZnO:Ga Thin Films at Room Temperature on Polymeric Substrates: Thickness Dependence," *Thin Solid Films*, **442**, 121–6 (2003).
- <sup>21</sup>D. R. Sahu and J. L. Huang, "The Properties of ZnO/Cu/ZnO Multilayer Films Before and After Annealing in the Different Atmosphere," *Thin Solid Films*, **516**, 208–11 (2007).
- <sup>22</sup>C. H. Tseng, C. H. Huang, H. C. Chang, D. Y. Chen, C. P. Chou, and C. Y. Hsu, "Structural and Optoelectronic Properties of Al-Doped Zinc Oxide Films Deposited on Flexible Substrates by Radio Frequency Magnetron Sputtering," *Thin Solid Films*, **519**, 7959–65 (2011). □